Science 2016 Aug 5;353(6299):587-90. doi: 10.1126/science.aaf9793.

Title: Circadian regulation of sunflower heliotropism, floral orientation, and pollinator visits

Authors: Hagop S. Atamian[1], Nicky M. Creux[1], Evan A. Brown[2], Austin G. Garner[2], Benjamin K. Blackman[2,3], and Stacey L. Harmer[1*]

Affiliations:

[1]Department of Plant Biology, University of California, One Shields Avenue, Davis, CA 95616, USA.

[2]Department of Biology, University of Virginia, PO Box 400328, Charlottesville, VA 22904, USA.

[3]Department of Plant and Microbial Biology, University of California, 111 Koshland Hall, Berkeley, CA 94720, USA.

*Correspondence to: slharmer@ucdavis.edu.

Abstract:

Young sunflower plants track the sun from east to west during the day and then reorient during the night to face east in anticipation of dawn. In contrast, mature plants cease movement with their flower heads facing east. We show that circadian regulation of directional growth pathways accounts for both phenomena and leads to increased vegetative biomass and enhanced pollinator visits to flowers. Solar tracking movements are driven by antiphasic patterns of elongation on the east and west sides of the stem. Genes implicated in control of phototropic growth, but not clock genes, are differentially expressed on the opposite sides of solar tracking stems. Thus interactions between environmental response pathways and the internal circadian oscillator coordinate physiological processes with predictable changes in the environment to influence growth and reproduction.

One Sentence Summary:

Sun-tracking when young, east-facing when mature, warmer sunflowers attract more pollinators.

Text+References+Legends

Cover

Main Text:

Most plant species display daily rhythms in organ expansion that are regulated by complex interactions between light and temperature sensing pathways and the circadian clock (*1*). These rhythms arise in part because the abundance of growth-related factors such as light signaling components and hormones such as gibberellins and auxins are regulated both by the circadian clock and light (*2-4*). A further layer of regulation is afforded by circadian gating of plant responsiveness to these stimuli, with maximal sensitivity to light during the day (*5*) and to gibberellin and auxin at night (*6, 7*).

Since the direction and amount of solar irradiation undergo predictable daily changes, light capture might be optimized by links between the circadian clock and directional growth pathways. One such growth pathway is phototropism, in which plants align their photosynthetic organs with the direction of incoming light. Phototropism was first recognized by Charles Darwin (*8*), and is mediated by the perception of blue light by phototropin photoreceptors that then trigger asymmetric growth via the auxin signaling pathway (*9*). Heliotropism, or solar tracking, is a more dynamic form of phototropism, with aerial portions of the plant following the sun's movement throughout the day. Some heliotropic plants such as sunflowers also reorient during the night so that leaves and apices face east prior to sunrise (*10, 11*). Here, we show that heliotropism in the common sunflower, *Helianthus annuus*, is generated by the coordinate action of light signaling pathways and the circadian clock and enhances plant performance in the natural environment.

Sunflower stems exhibit heliotropic movement such that their shoot apices shift from facing east at dawn to facing west at dusk as they track the sun's relative position. Shoot apices then reorient at night to face east in anticipation of dawn (Fig. 1A and movie S1) (*12, 13*). We disrupted this process in two ways, either rotating potted plants every evening so that they faced east at nightfall (and thus faced west each morning after directional nighttime growth), or tethering the stems of plants to solid supports to limit their tracking movements. In multiple trials, we found approximately 10% decreases in both dry biomass and leaf area of the manipulated plants relative to controls in both types of experiments (Fig. 1B; fig. S1; significance assessed using linear mixed-effect models with treatment as fixed effect, trial and leaf number as random effects), demonstrating that solar tracking promotes growth.

The nighttime reorientation of young sunflowers in the absence of any obvious environmental signal suggests involvement of the circadian system; however, an alternative explanation would be an hourglass-like timing mechanism. To distinguish between these possibilities, we examined the kinetics of nighttime reorientation near the summer solstice and the fall equinox. The rate of apical movement at night was higher at midsummer (16 h light: 8 h dark, 16L:8D) than during the longer nights of autumn (12L:12D) so that in each case plant apices face fully east just before dawn (Fig. 1C). We next investigated whether plants continue rhythmic tracking movements in the absence of directional light cues. Sunflower plants grown in pots in the field in 14L:10D conditions were heliotropic (Fig. 1D). When moved to a growth chamber with constant, fixed overhead lighting, these plants maintained their directional growth rhythms for several days. Plants reoriented towards the east during the subjective night and towards the west during the subjective day, with times of maximal inclination corresponding to

subjective dawn and dusk. As is true for many types of circadian outputs after withdrawal of environmental signals, rhythmic movements dampened over time (Fig. 1D).

Another way to distinguish rhythms regulated by the circadian clock from those directly induced by environmental cues is to maintain organisms in light/dark cycles with total period lengths (T-cycles) differing from 24 h (*14*). We examined heliotropism in a growth chamber with four directional blue LED lights sequentially turned on and off to mimic the sun's daily path. After several days in a 24 h T-cycle (16L:8D), plants bent towards light during the day so that 'westward' movement culminated at dusk. Anticipatory 'eastward' movement then occurred throughout the dark period (Fig. 1E and fig. S2). Upon transfer to a 30 h T-cycle (20L:10D), maximal 'westward' inclination no longer occurred at the light/dark transition and directionality of nighttime movement was erratic. Return to 24 h T-cycles reestablished anticipatory nighttime movement beginning at lights off (Fig. 1E and fig. S2). The complex patterns in 30 h T-cycles suggest uncoordinated growth controlled by both environmental response pathways and the circadian clock. Thus the circadian clock guides solar tracking in sunflower.

Because sunflowers lack pulvini, the specialized motor organs that mediate solar tracking in some species (*15*), we hypothesized that regulated stem elongation might drive solar tracking. Indeed, we observed a gradual reduction in amplitude of heliotropic movements as plants reach maturity, correlating with cessation of stem elongation (Fig. 3A). To further investigate the involvement of stem elongation in heliotropism, we examined solar tracking and stem growth rates in *dwarf2* (*dw2*) sunflowers, which are deficient in production of gibberellin growth hormones (*16*). In the absence of exogenous gibberellin, *dw2* plants have very short stems and no perceptible heliotropism (movie S2). Treatment with exogenous gibberellin transiently restored normal elongation (Fig. 2A) as well as heliotropism (Fig. 2B) in the mutant. Between days 7 and 14 after the last gibberellin application, stem elongation and the amplitude of solar tracking rhythms coordinately diminished by about 35% (Fig. 2A and 2B). Thus stem elongation is essential for heliotropism.

Many plant species show daily rhythms in non-directional stem and leaf growth (*1*). We hypothesized that heliotropism results from differential elongation on opposite sides of stems. Indeed, the growth pattern on the east side of solar tracking sunflower stems was different from that on the west side (Fig. 2C). Growth rates on the east side were high during the day and very low at night, whereas growth rates on the west side were low during the day and higher at night. The higher growth rate on the east compared to the west side of the stem during the day enables the shoot apex to move gradually from east to west. At night, the higher growth rate on the west compared to the east side culminates in the apex facing east at dawn. We postulated that one of these growth patterns might be similar to the overall growth rhythms of sunflower plants not manifesting heliotropism. We therefore monitored plants maintained in 16L:8D cycles in a growth chamber with overhead lighting. Consistent with reports in pea and zinnia (*17, 18*), stem elongation growth rates were higher at night than during the day under these controlled conditions (Fig. 2D), resembling the growth pattern of the west side of solar tracking stems. These data suggest that heliotropism is mediated by the default pattern of growth on the west sides of stems combined with a novel growth pattern, imposed by environmental factors, on the east sides.

Because our data implicate the circadian clock in solar tracking movements, we examined the expression of sunflower homologs of central clock genes on the east and west sides of solar tracking stems. Although a *LATE ELONGATED HYPOCOTYL*-like and a *TIMING OF*

CAB EXPRESSION1-like gene displayed the expected rhythmic patterns of daily expression, they were not differentially expressed on the opposite sides of stems (Fig. 2E and 2F). However, expression of two homologs of genes implicated in phototropism (*19, 20*) differed on the opposite sides of solar tracking sunflower stems, with an *INDOLE-3-ACETIC ACID19*-like gene more highly expressed on the west side at night (Fig. 2G) and a *SMALL AUXIN-UPREGULATED50 (SAUR50)*-like gene more highly expressed on the east side during the day (Fig. 2H). Homologs of these genes are induced by auxin in many species (*21*) and SAUR proteins promote cell elongation (*22*). Directional growth towards a light source is thought to be instigated by the phototropin-triggered redistribution of auxin across plant stems (*9*), while the circadian clock regulates both auxin levels and plant responsiveness to exogenous auxin (*4, 7*). We think it plausible that solar tracking rhythms are generated by coordinate regulation of auxin signaling by blue light photoreceptors and the circadian clock on the opposite sides of a radially symmetrical organ, the sunflower stem.

In nature, only young sunflower plants exhibit heliotropic movements. At the final stage of floral development, or anthesis, sunflower apices stop tracking the sun and acquire a permanent eastward orientation (*12*). Close examination of the growth dynamics over this period revealed that as stem elongation slows, likely accounting for the overall reduction in movement, the apices move less and less to the west each day, although they return to face east by morning (Fig. 3A and movie S3). This gradual cessation of westward movement might be explained by circadian gating of plant responsiveness to light, with plants responding more strongly to activation of the phototropin blue-light photoreceptors in the morning than at other times of day. We tested this possibility by entraining young plants in 16L:8D cycles and measuring their bending response following exposure to unidirectional blue light at different times of the day or night. Plants exposed to light during the first part of the day showed a stronger tropic response than those stimulated late in the day or at night (Fig. 3B), consistent with studies in potato (*23*). These data suggest that lower competence of plants to respond to directional light in the afternoons and evenings (Fig. 3B) combined with progressively reduced elongation rates as plants approach maturity likely accounts for the progressive loss of daily stem movements towards the west and can explain the eastward orientation of sunflower disks at anthesis.

We next investigated whether this eastward orientation provides any ecological advantage. Since floral orientations that elevate floral temperature enhance pollinator visitation in alpine plants (*24, 25*), we hypothesized that an eastward orientation may promote sunflower attractiveness to pollinators through increased morning interception of solar radiation, coincident with the daily timing of anther and stigma exsertion. Sunflowers were grown in pots in the field, and just before the appearance of ray petals, half were rotated to face west. Hourly recording of disk temperature by forward-looking infrared (FLIR) imaging and more continuous monitoring with thermocouples revealed that east-facing heads warmed up more quickly in the morning than west-facing heads (Fig. 3C; fig. S3). In these early-morning hours, pollinators visited east-facing heads fivefold more often than west-facing heads (Fig. 3D). This differential was observed only at times when east-facing flowers were warmer than west-facing flowers. With the exception of one trial where plants flowered during a period of inclement weather, these observations were consistent across trials, years, and field sites (fig. S3). Notably, west-facing flowers warmed with portable heaters so that their morning surface temperatures matched east-facing flowers received significantly more pollinator visits than non-heated west-facing flowers (Fig. 3E-F; fig. S3F-G), albeit fewer than east-facing flowers. Thus temperature directly contributes to, but does not solely determine, the differential attractiveness of east- and west-facing flowers to pollinators. In

the future, we will investigate how temperature affects floral physiology and interactions with pollinators.

Circadian oscillators enhance fitness by coordinating physiological processes with predictable changes in the environment (*26, 27*). Our findings demonstrate that such impacts accrue in part through the coordinate regulation of directional growth by environmental response pathways and the circadian oscillator. Such coordination generates the heliotropic movement of young sunflowers, enhancing plant growth, and also leads to the eastward orientation of blooming sunflower disks, promoting a key component of reproductive performance.

References

1. L. M. Muller, M. von Korff, S. J. Davis, Connections between circadian clocks and carbon metabolism reveal species-specific effects on growth control. *J. Exp. Bot.* **65**, 2915-2923 (2014).
2. K. Nozue *et al.*, Rhythmic growth explained by coincidence between internal and external cues. *Nature* **448**, 358-361 (2007).
3. K. R. Foster, P. W. Morgan, Genetic Regulation of Development in Sorghum bicolor (IX. The ma3R Allele Disrupts Diurnal Control of Gibberellin Biosynthesis). *Plant Phys.* **108**, 337-343 (1995).
4. L. Jouve, T. Gaspar, C. Kevers, H. Greppin, R. Degli Agosti, Involvement of indole-3-acetic acid in the circadian growth of the first internode of Arabidopsis. *Planta* **209**, 136-142 (1999).
5. A. J. Millar, S. A. Kay, Integration of circadian and phototransduction pathways in the network controlling *CAB* gene transcription in *Arabidopsis*. *Proc. Natl. Acad. Sci. U.S.A.* **93**, 15491-15496 (1996).
6. M. V. Arana, N. Marin-de la Rosa, J. N. Maloof, M. A. Blazquez, D. Alabadi, Circadian oscillation of gibberellin signaling in Arabidopsis. *Proc. Natl. Acad. Sci. U.S.A.* **108**, 9292-9297 (2011).
7. M. F. Covington, S. L. Harmer, The circadian clock regulates auxin signaling and responses in Arabidopsis. *PLoS Biol.* **5**, e222 (2007).
8. C. R. Darwin, *The power of movement in plants*. (John Murray, London, 1880).
9. W. R. Briggs, Phototropism: some history, some puzzles, and a look ahead. *Plant Phys.* **164**, 13-23 (2014).
10. J. P. Vandenbrink, E. A. Brown, S. L. Harmer, B. K. Blackman, Turning heads: the biology of solar tracking in sunflower. *Plant Sci.* **224**, 20-26 (2014).
11. U. Kutschera, W. R. Briggs, Phototropic solar tracking in sunflower plants: an integrative perspective. *Ann. Bot.* **117**, 1-8 (2016).
12. J. H. Schaffner, Observations on the nutation of Helianthus annuus. *Bot. Gaz.* **25**, 395-403 (1898).
13. H. Shibaoka, T. Yamaki, Studies on the growth movement of sunflower plant. *Sci. Pap. Coll. Gen. Educ. Univ. Tokyo* **9**, 105-126 (1959).
14. M. Merrow, M. Brunner, T. Roenneberg, Assignment of circadian function for the Neurospora clock gene frequency. *Nature* **399**, 584-586 (1999).
15. D. Koller, in *Photo-movement,* D.-P. Häder, M. Lebert, Eds. (Elsevier, Amsterdam, 2001), pp. 833-896.
16. M. Fambrini *et al.*, The extreme dwarf phenotype of the GA-sensitive mutant of sunflower, dwarf2, is generated by a deletion in the ent-kaurenoic acid oxidase1 (HaKAO1) gene sequence. *Plant Mol. Biol.* **75**, 431-450 (2011).
17. J. A. Stavang *et al.*, Thermoperiodic stem elongation involves transcriptional regulation of gibberellin deactivation in pea. *Plant Phys.* **138**, 2344-2353 (2005).
18. W. G. Neily, P. R. Hickelton, D. N. Kristie, Temperature and developmental stage influence diurnal rhythms of stem elongation in snapdragon and zinnia. *J. Am. Soc. Hort. Sci.* **122**, 778-783 (1997).
19. H. Ren, W. M. Gray, SAUR Proteins as Effectors of Hormonal and Environmental Signals in Plant Growth. *Mol. Plant* **8**, 1153-1164 (2015).

20. K. Tatematsu *et al.*, MASSUGU2 encodes Aux/IAA19, an auxin-regulated protein that functions together with the transcriptional activator NPH4/ARF7 to regulate differential growth responses of hypocotyl and formation of lateral roots in Arabidopsis thaliana. *Plant Cell* **16**, 379-393 (2004).
21. G. Hagen, T. Guilfoyle, Auxin-responsive gene expression: genes, promoters and regulatory factors. *Plant Mol. Biol.* **49**, 373-385 (2002).
22. A. K. Spartz *et al.*, SAUR Inhibition of PP2C-D Phosphatases Activates Plasma Membrane H+-ATPases to Promote Cell Expansion in Arabidopsis. *Plant Cell* **26**, 2129-2142 (2014).
23. D. Vinterhalter, B. Vinterhalter, J. Miljuš-Djukić, Ž. Jovanović, V. Orbović, Daily changes in the competence for photo- and gravitropic response by potato plantlets. *J. Plant Growth Reg.* **33**, 539-550 (2014).
24. P. G. Kevan, Sun-tracking solar furnaces in high arctic flowers: significance for pollination and insects. *Science* **189**, 723-726 (1975).
25. M. L. Stanton, C. Galen, Consequences of flower heliotropism for reproduction in an alpine buttercup (*Ranunculus adoneus*). *Oecol.* **78**, 477-485 (1989).
26. Y. Ouyang, C. R. Andersson, T. Kondo, S. S. Golden, C. H. Johnson, Resonating circadian clocks enhance fitness in cyanobacteria. *Proc. Natl. Acad. Sci. U.S.A.* **95**, 8660-8664 (1998).
27. A. N. Dodd *et al.*, Plant circadian clocks increase photosynthesis, growth, survival, and competitive advantage. *Science* **309**, 630-633 (2005).
28. A. A. Schneiter, J. F. Miller, Description of sunflower growth stages. *Crop Sci.* **21**, 901-903 (1981).
29. C. A. Schneider, W. S. Rasband, K. W. Eliceiri, NIH Image to ImageJ: 25 years of image analysis. *Nat. Methods* **9**, 671-675 (2012).
30. D. Bates, M. Maechler, B. Bolker, S. Walker, Fitting linear mixed-effects models using lme4. *J. Stat. Softw.* **67**, 1-48 (2015).
31. A. Kuznetsova, P. B. Brockhoff, R. H. B. Christensen, lmerTest: Tests in Linear Mixed Effects Models. R package version 2.0-30. https://CRAN.R-project.org/package=lmerTest, (2016).
32. R. C. Team, R: A language and environment for statistical computing. *R Foundation for Statistical Computing* https://www.R-project.org/, (2015).
33. E. L. Martin-Tryon, J. A. Kreps, S. L. Harmer, GIGANTEA acts in blue light signaling and has biochemically separable roles in circadian clock and flowering time regulation. *Plant Phys.* **143**, 473-486 (2007).
34. J. Vandesompele *et al.*, Accurate normalization of real-time quantitative RT-PCR data by geometric averaging of multiple internal control genes. *Genome Biol.* **3**, RESEARCH0034 (2002).
35. M. V. Matz, MCMC.qpcr: Bayesian analysis of qRT-PCR data. R package version 1.2.2. https://CRAN.R-project.org/package=MCMC.qpcr (2015).

Acknowledgments: We thank C. Pugliesi and the USDA (ARS, NCRPIS) for providing germplasm; the Morven Farm staff, R. Karp, J. Vandenbrink, L. Henry, and N. Infantino for assistance in the field and with video scoring; and J. Maloof for helpful discussions. This work was supported by National Science Foundation grant IOS-1238040 (to S.L.H.

and B.K.B.) and a UVA Harrison Undergraduate Research Award (to E.A.B.).
Supplement contains additional data.

Supplementary Materials:

Materials and Methods

Table S1

Figures S1 - S3

References (28 - 35)

Movies S1 – S3

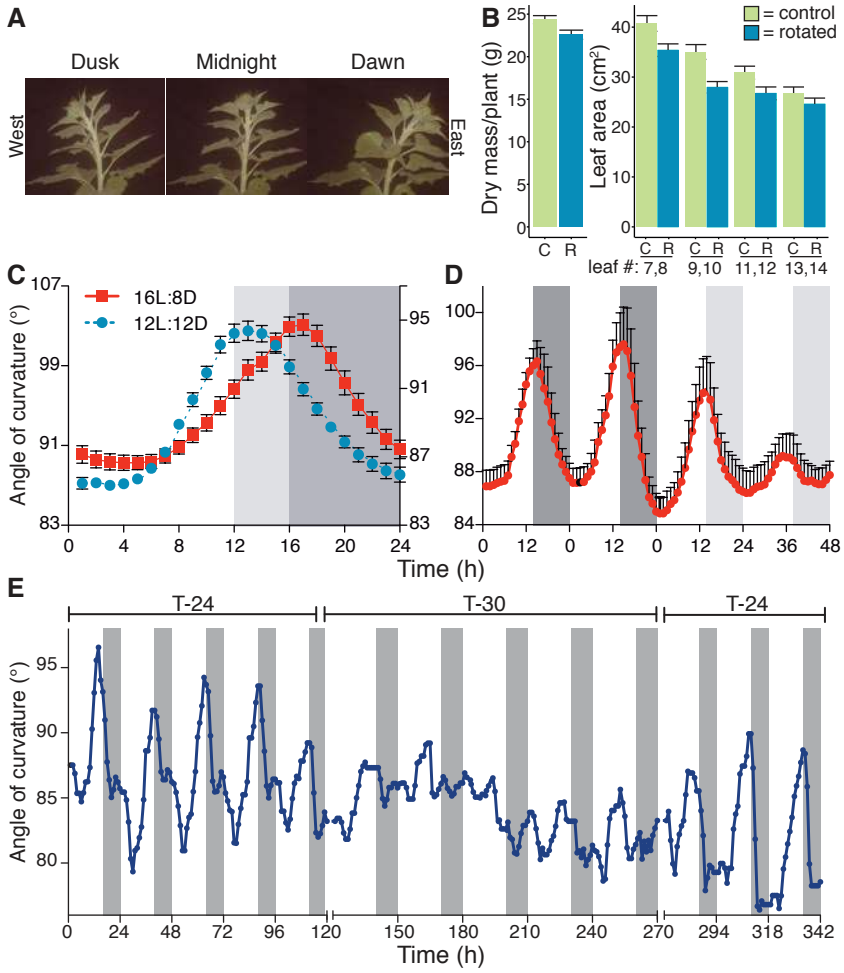

Fig. 1. **The circadian clock regulates solar tracking**. (**A**) Nighttime reorientation of stem and shoot apex. (**B**) Disruption of solar tracking by daily evening 180° rotation of experimental plants results in a 7.5% reduction in biomass (left) and an 11% reduction in leaf area (right) compared to 360º rotated control plants (mean ± s.e.m., n=80, p = 0.01 and $1e^{-6}$, respectively, mixed effect linear regression models). Numbers refer to leaf pairs. (**C**) Changes in orientation anticipate dawn and dusk transitions both in fall (primary y-axis) and summer (secondary y-axis) (mean ± s.e.m., n=10). (**D**) Persistence of rhythmic movements following transfer from field to continuous light and temperature conditions. Dark and light grey areas represent night and subjective night, respectively (mean ± s.e.m., n=3). (**E**) The onset of 'eastward' movement in a growth chamber equipped with 4 directional lights is consistently phased to lights off in 24 h T-cycles (left and right) but is erratic in 30 h T-cycles (center). Time 0 indicates dawn (**C, D**) or the beginning of the first T-cycle (**E**). Angles <90º and >90º represent inclination towards east and west, respectively. White areas = day, grey = night.

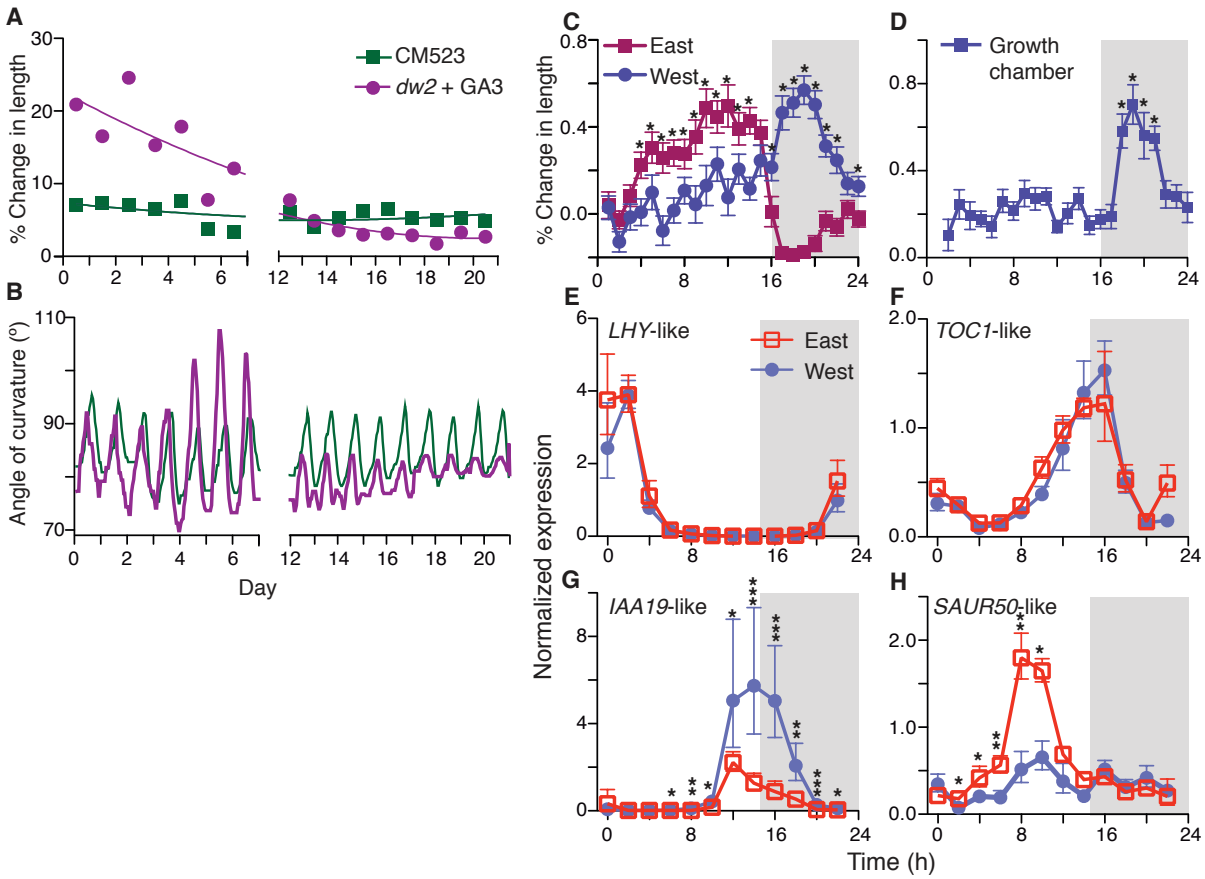

Fig. 2. Solar tracking is driven by opposing growth rhythms on the east and west sides of stems. (**A**) Changes in stem elongation and (**B**) the angle of curvature of the shoot apex relative to the horizon in control and gibberellin-deficient *dw2* plants. *dw2* mutants were treated twice with 2 μM of the gibberellin GA_3, with the last treatment on day 0. Data in (**A**) were fitted to centered second order polynomial equations to aid visualization. (**C**) Timing of elongation of the east and west sides of stems of solar tracking field-grown plants (mean ± s.e.m., n=42). (**D**) Timing of stem elongation of plants growing vertically in a top-lit environmental control chamber (mean ± s.e.m., n = 9). Asterisks indicate that the east and west sides of the stem (**C**) or the daytime and nighttime means (**D**) significantly differ (*$p < 0.05$, Student's t-test). (**E - H**) Differential gene expression on the east and west sides of solar tracking stems assessed by qRT-PCR (*$p < 0.05$, **$p < 0.01$, ***$p < 0.001$, orientation by timepoint effect, single linear mixed model). Time 0 indicates dawn (**C; E - H**) or lights on (**D**). White areas = day, grey = night.

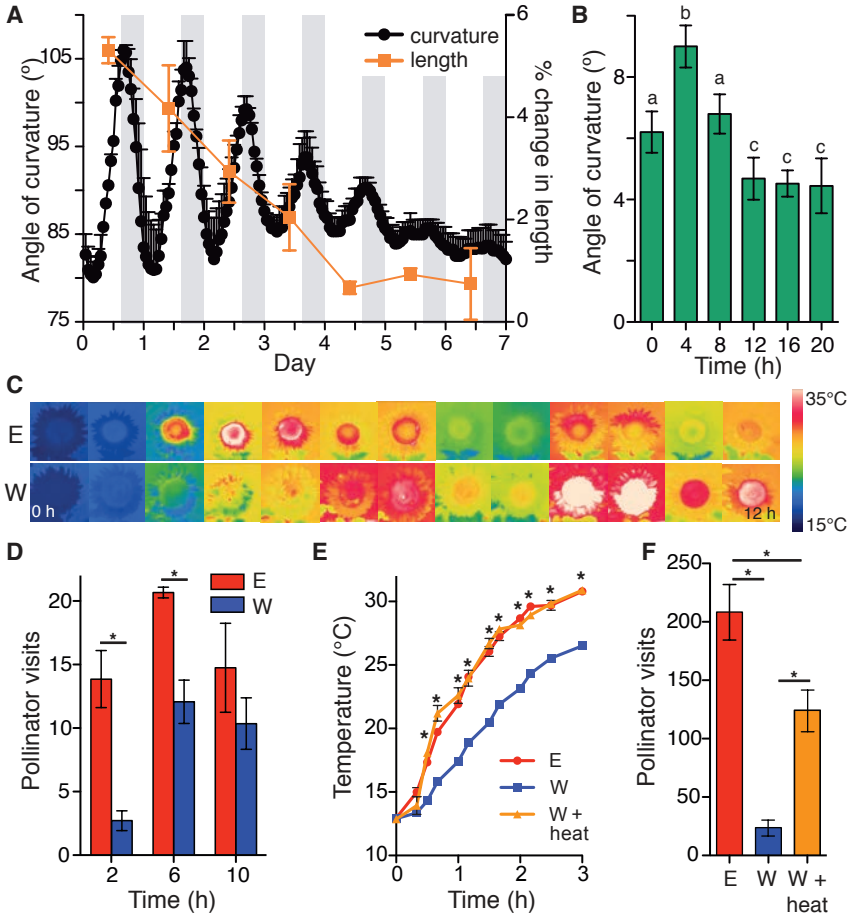

Fig. 3. Eastward orientation of sunflower heads after anthesis is due to gating of light responses by the circadian clock and enhances pollinator visits. (**A**) Amplitude of solar tracking and changes in stem growth of mature plants nearing floral anthesis. Petals were first observed during day 5 (mean ± s.e.m., n=2). (**B**) Stem curvature of juvenile plants entrained in 16L:8D cycles and then exposed to unidirectional blue light for 4 h at the indicated times (mean ± s.e.m., n=11). Different letters indicate significantly different curvature values in pairwise comparisons. $p < 0.05$, Student's t-test. (**C**) FLIR images of east-facing (E) and west-facing (W) floral disks at hourly intervals. (**D**) Pollinator visits to E and W plants (mean ± s.e.m., n=4 days, 8 plants per treatment) during 45 minute intervals at three times of day. (**E**) Temperature (mean ± s.e.m., n=6 per condition) of sunflower disks with east or west orientations (with or without supplemental heat). (**F**) Pollinator visits in the morning to the inflorescences with temperatures reported in **E**. *$p < 0.05$ (W vs W+heat; t-test with unequal variances. Time zero indicates dawn (**A**, **C** – **E**) or lights on (**B**).

Science 2016 Aug 5;353(6299):587-90. doi: 10.1126/science.aaf9793.

Supplementary Materials for

Circadian regulation of sunflower heliotropism, floral orientation, and pollinator visits

Hagop S. Atamian, Nicky M. Creux, Evan A. Brown, Austin G. Garner, Benjamin K. Blackman, and Stacey L. Harmer.

correspondence to: slharmer@ucdavis.edu

This PDF file includes:

Other Supplementary Materials for this manuscript includes the following:

Materials and Methods

Plant materials and growth conditions

Seeds of HA412-HO (USDA Germplasm Resources Information Network ID: PI 603993) were provided by the USDA, ARS, and NCRPIS (Iowa State University). Wild-type (inbred line CM523) and *dwarf2* (*dw2*) seeds were kindly provided by Claudio Pugliesi (University of Pisa, Italy). Seeds of the Sunspot variety were purchased from Botanical Interests, Inc. Seeds were sown in SunGro® Sunshine® mix #1 and germinated in a growth chamber in the dark for 3 days. They were then either kept in an environmental chamber under 16L:8D (200 $\mu mol\ m^{-2}\ s^{-1}$ fluorescent light) at 24°C or transplanted to the field two days post-germination.

For investigating the sunflower heliotropic response under constant light conditions, two-day-old seedlings (Sunspot variety) were transplanted to pots and kept in an open greenhouse with no artificial lighting. At the early R1 stage of development (*28*), the pots were moved to a growth chamber at dawn and kept for two days under constant temperature and constant dim light (5 $\mu mol\ m^{-2}\ s^{-1}$, light provided by cool white fluorescent bulbs).

For examining the sunflower heliotropic response under different light/dark cycles, seedlings (Sunspot variety) were grown in growth chambers (described above). At the V10 stage of development (*28*), plants were moved to a growth chamber with an artificial light system, with four blue LED lights arranged in an arc that were sequentially turned on and off to mimic the motion of the sun. Background overhead incandescent light was also provided during the light period. Plants were maintained in 24 h, 30 h, or 32 h T-cycles in which each light was turned on for either 4 h or 5 h to generate 16L:8D, 20L:10D, or 16L:16D conditions.

For defining the growth pattern of sunflower stems in a growth chamber illuminated from above with fluorescent white light (200 $\mu mol\ m^{-2}\ s^{-1}$; 16L:8D), V6 stage (*28*) plants (Sunspot and HA412-HO varieties) were used. Photographs were taken using BirdCam 2.0 (Wingscapes®) cameras. The length of the sunflower stem was measured every hour from the apex to the base of the stem using ImageJ (*29*) software.

For measuring the growth patterns on opposite sides of the stem, HA412-HO plants were grown in the field under long day conditions. Time-lapse photography was carried out using BirdCam 2.0 cameras. The lengths on opposite sides of the stem were measured by tracing the edges of the stem between two marks at the base and the apex of each side of the stems using ImageJ software.

The *dw2* mutant plants were genotyped as previously described (*16*). Two week-old mutant plants were sprayed twice with 2 $\mu M\ GA_3$ in 0.05% Tween-20 (three days apart) while the wild type was sprayed with 0.05% Tween-20 as control.

For quantification of heliotropism, images of sunflower plants were taken every hour using BirdCam 2.0 cameras (both for plants grown in the field and in growth chambers) and the angle of curvature of the apex relative to the horizon line was measured over 24 h using ImageJ. Angles greater than 90° represent orientation towards the west and angles less than 90° represent orientation towards east.

Two approaches were used to disrupt heliotropism. In the first approach, HA412-HO plants were grown in two-gallon pots in the field and rotated either 180° (treatment) or 360° (control) at sunset for two months. In the second approach, HA412-HO plants were grown in the field and either their stems were tethered to solid supports to limit their tracking movements (treatment) or left free to track (control). Leaves 7 - 14 of the rotated plants and leaves 9 - 18 of the tethered plants were photographed and their area measured using ImageJ software. At end of the season,

plant stems and leaves were harvested, dried for five days at 140 ^{o}C and weighed to determine biomass. Statistical significance was assessed using the lme4 (*30*) and the lmerTest (*31*) packages in the R statistical environment (*32*).

For an examination of gating of light responses by the circadian clock, sunflower seedlings (Sunspot variety) were entrained in 16L:8D periods with cool white fluorescent bulbs. Two weeks after germination, they were subjected to unidirectional blue light (80 μmol m^{-2} s^{-1}) for 4 h at different times of the day and night and images were acquired using BirdCam 2.0 cameras. The angle of curvature of the apex relative to the horizon was measured at the end of each 4 h interval using ImageJ software.

All experiments were repeated at least twice.

Expression analysis

For gene expression analysis, HA412-HO plants were seeded in pots and transplanted to the field three days after germination. Two weeks later, the stem between the cotyledon and the first internode was longitudinally cut in half at the indicated time points. RNA was extracted from the east and west side of the harvested stems using the TRIzol protocol (Invitrogen) followed by on-column DNase treatment and cleaning through Spectrum™ Plant Total RNA Kit. cDNA was synthesized from 500 ng of total RNA using SuperScriptase III (Invitrogen). qRT-PCR was performed as previously described (*33*). Five independent biological samples were analyzed in technical triplicates using CFX96 Touch™ Real Time PCR machine (Bio-Rad, Hercules, CA). Expression of genes of interest were normalized to the geometric mean of the expression levels of four reference genes (*34*) using the R package MCMC.qpcr (*35*). Primers and gene sequences are listed in Table S1.

Pollinator visits

Two experiments were completed in Davis, CA in August and September 2014, and three experiments were completed in summers 2013 and 2014 at Morven in Charlottesville, VA. Seeds of accession HA412-HO were initially sown in cell packs (6x4x6 cm) and later transplanted into five-gallon paint buckets. At anthesis, pots were rotated to form two groups, one facing east and one facing west (2013: n = 5 plants per group; 2014: n = 8 at Morven and n= 4 plants in Davis) and were left in these orientations for the duration of the experiment. Each group was filmed with a Flip UltraHD Video Camera (Cisco Systems Inc., San Jose, CA) for 45 minutes at 8:00 am, 12:00 pm, and 4:00 pm in Virginia and with a Bloggie touch mobile HD snap camera (Sony) for 30 minutes at 9:00 am, 1:00 pm and 5:00 pm in Davis. The total number of pollinator visits was manually counted in each video for each plant in each direction using Bloggie touch software (Sony) or VLC Media Player (VideoLan Organization) for viewing. All insect visitors that were large enough to be visible on the face of the flower were counted regardless of species. A new visit was counted when an insect entered the frame of the video and landed on the flower face. If multiple heads were in frame, movement between heads was counted toward total visits. The average number of initial or total visits per plant was calculated by treatment for each recording interval each day. For each time interval observed, a t-test assuming unequal variances comparing east vs. west treatment means across days observed was performed in Excel.

Temperature measurements

Floral head temperatures were assessed with two methods: forward-looking infrared (FLIR) imaging at regular daytime intervals and more continuous logging using thermocouples. At

Morven, infrared images of heads with open disk florets were taken using a FLIR Exx-series infrared camera (model FLIR i7; FLIR Systems, Inc., Wilsonville, OR) hourly from 06:30 to 18:30 over a three-day period in 2013 (n = 5 plants) or hourly from 06:00 to 18:00 over a four-day period in 2014 (n = 8). Images were analyzed with FLIR Tools (version 4.0.13330.1003). To determine the average surface temperature of a plant at a given time, the floral disk was manually outlined with a selection tool and the mean temperature reported for the area selected was recorded. For each time point for each plant, the average across days was calculated.

At both Morven and Davis, RDXL4SD data loggers and K-type copper-constantan thermocouples (Omega engineering) were used to measure the flower head temperature. Thermocouple probes were inserted into the center of the face of east and west facing HA412-HO sunflowers and temperatures were logged every 10 minutes for 3 or 4 days. The temperatures were averaged across the four days. Ambient air temperature was measured using the HOBO Pro v2 data logger (Onset) for the same period. Head temperatures were standardized to ambient temperatures to control for temperature variation among days, and means across days ± s.e.m. for each time point were plotted in R. Because malfunction of the ambient data logger at Morven failed to record values for several intervals, some time points on some days were excluded for one trial. For the Morven supplemental heating experiment (see below), temperatures were logged every 5 minutes during the period from dawn through the period of filming.

Supplemental Heating Experiments

Six supplemental heating experiments were completed in Davis, CA in August and September 2015, and three supplemental heating experiments were completed in August 2015 at Morven. Plants were grown, manipulated so they faced either east or west, and filmed as described above. In addition to the east and west treatments (n = 6 plants per filming group at Morven; n = 6 individual plants at Davis), sets of west-facing plants were heated either with an electric dish heater (H-500, Optimus Enterprise Inc., Anaheim, CA; Davis) or a triple burner propane heater (MH45T; Mr. Heater, Inc., Cleveland, OH; Morven). Temperature matching with east-facing plants was achieved through monitoring disk temperatures with a FLIR ONE Thermal Imager for iPhone 5S (FLIR Systems, Inc.) and adjusting the energy input to the heater or the distance between the heater and the plant(s) accordingly. Head temperatures were recorded using thermocouples. Pollinator visits were scored and analyzed as described above.

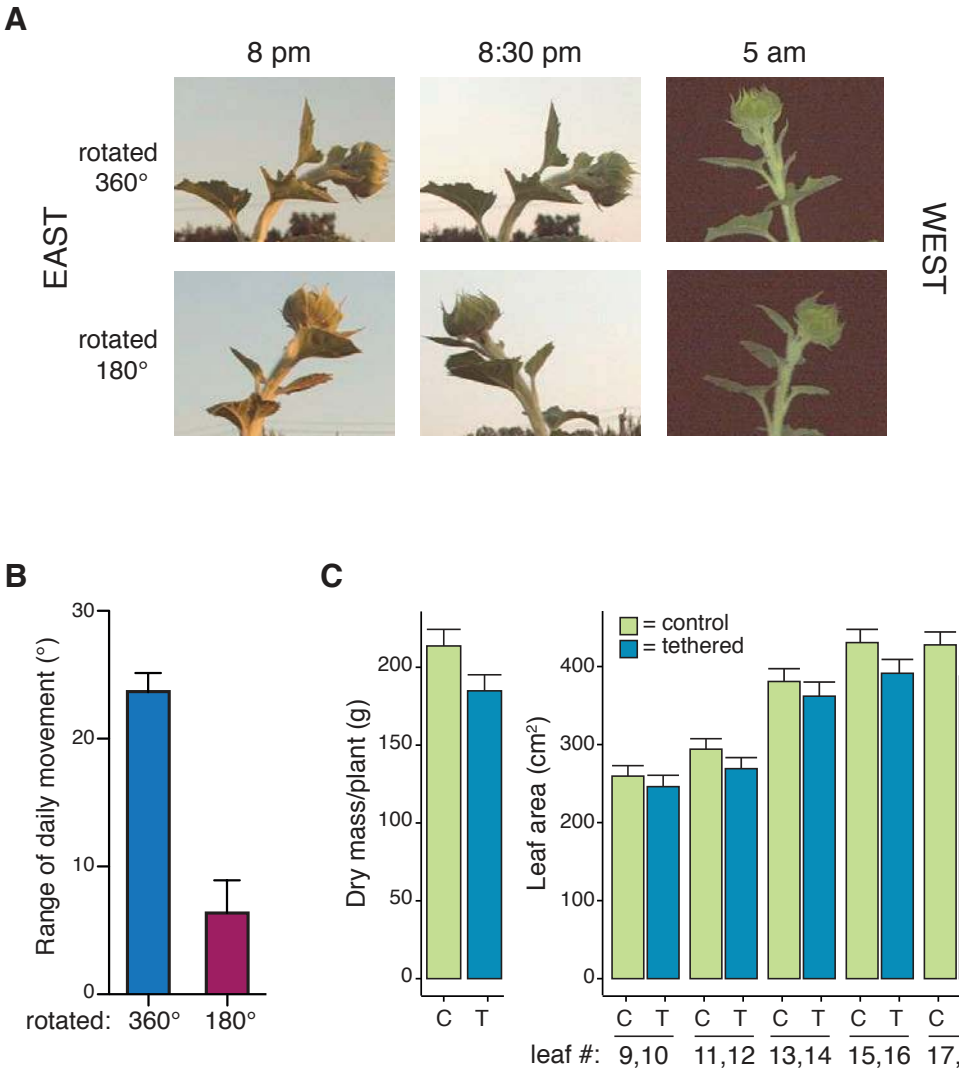

Fig. S1.

Disruption of solar tracking reduces growth. (**A**) In the rotation experiments, plants were grown in pots and every evening near sunset were either rotated 180° so that they faced east instead of west or were rotated 360° so that they still faced west. (**B**) The total range of daily stem bending movements (sunrise to sunset) of experimental plants is much smaller than that of control plants (mean ± s.e.m., n = 4; p = 0.001, Student's t-test). (**C**) Solar tracking of experimental plants was disrupted by securing stems to stakes with plant stretch tie tape. Experimental samples exhibited a 13% reduction in biomass (left) and an 9.7% reduction in leaf area (right) relative to the controls (mean ± s.e.m., n=83; p = 0.06 and 0.0092, respectively, mixed effect linear regression models with treatment as fixed effect, trial and leaf number as random effects). Numbers in the right panel refer to leaf pairs.

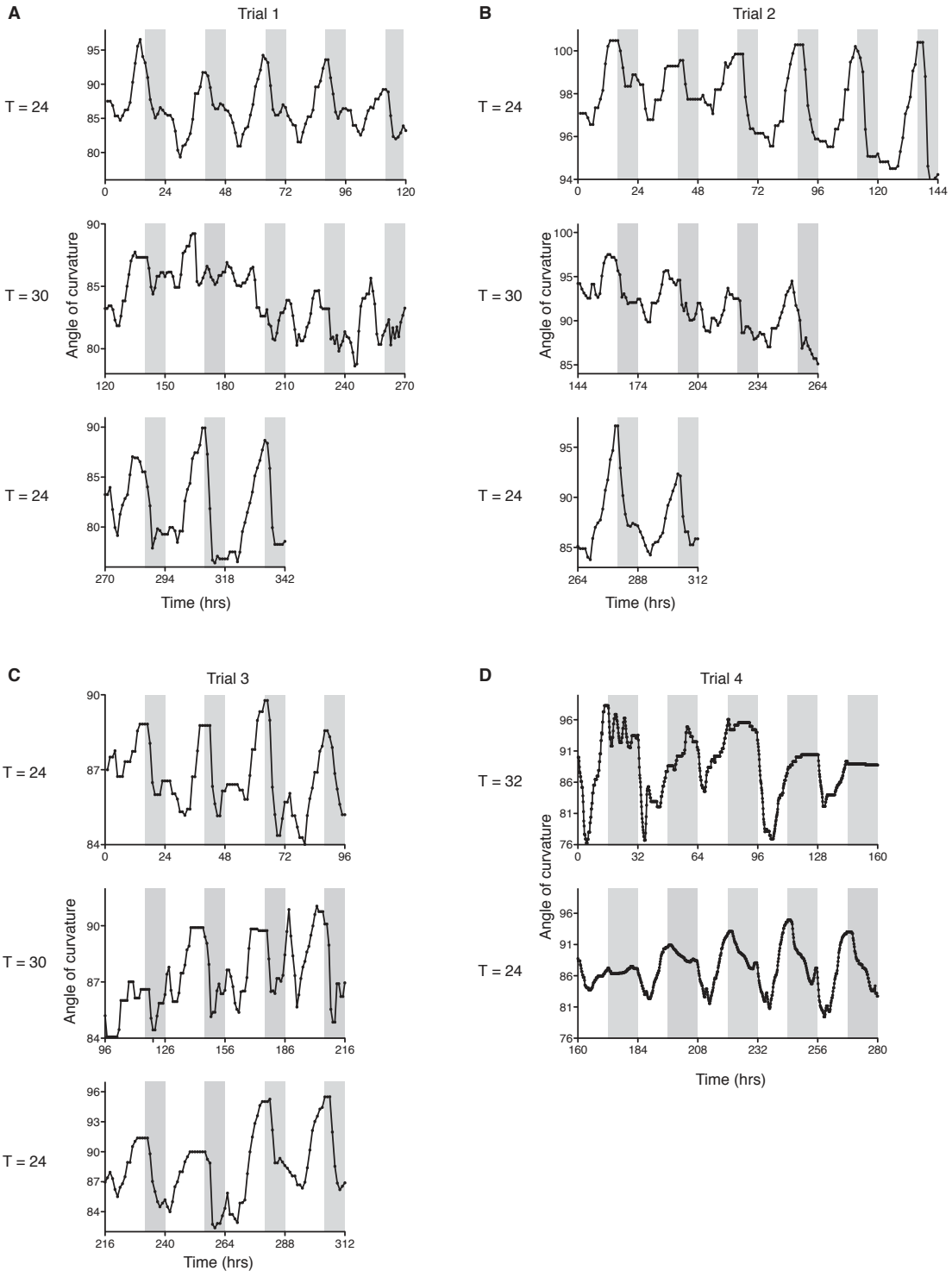

Fig. S2

Nighttime anticipatory growth is regulated by the circadian clock. Plants were monitored in a growth chamber with four directional lights sequentially turned on and off to mimic the sun's apparent movement. After several days of growth in the indicated T cycles (**A – C**) T = 24,

16L:8D; (**D**) T = 32, 16L:16D), plants were transferred to a new T cycle for several days (**A** - **C**, T = 30, 20L:10D; **D**, T = 24, 12L:12D). In **A** - **C**, plants were then transferred back to T = 24, 16L:8D. Time 0 indicates time directional light treatment was initiated. To facilitate comparisons, each T cycle is normalized so that it plotted over the same distance on the x axes.

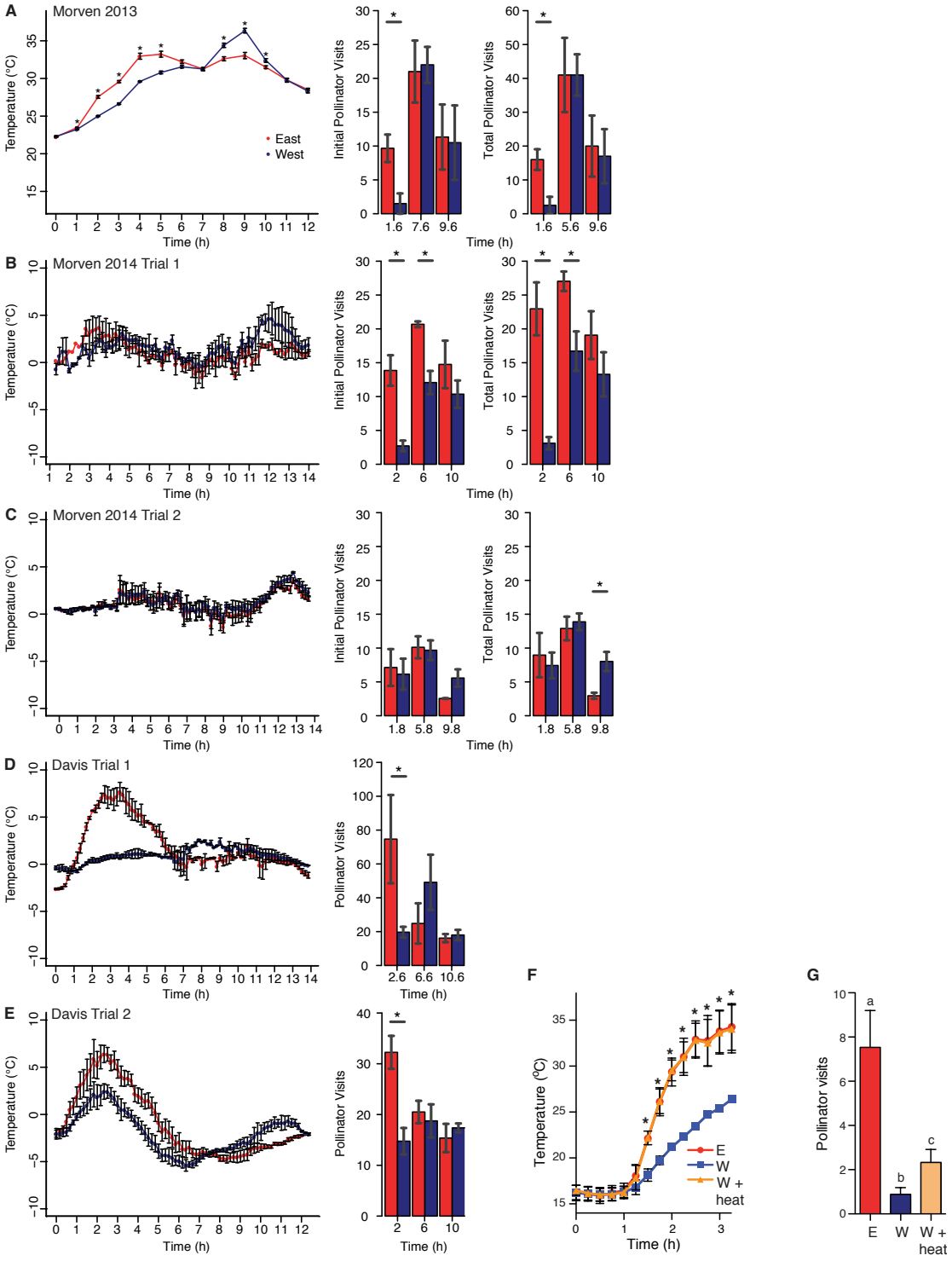
A
Morven 2013
Temperature (°C)
East
West
Time (h)
Initial Pollinator Visits
Total Pollinator Visits
1.6 7.6 9.6
1.6 5.6 9.6
B
Morven 2014 Trial 1
2 6 10
C
Morven 2014 Trial 2
1.8 5.8 9.8
D
Davis Trial 1
Pollinator Visits
2.6 6.6 10.6
E
Davis Trial 2
F
E
W
W + heat
G
a
b
c

Fig. S3

Daytime temperature profiles and pollinator visitations to east (red) and west (blue) facing sunflower heads over 6 trials across 2 locations. Trials were conducted in (A) August 2013, (B) mid-July 2014, (C) late-July 2014, and (F – G) mid-August 2015 at Morven in Albemarle County, Virginia and in (D) August 2014 and (E) September 2014 in Davis, California. In (A) mean temperature of the floral face of heads over three days ± s.e.m. as measured by FLIR is plotted hourly against time (h after dawn; n = 5 plants). Significant differences in mean head temperature between treatments, as determined by a Kruskal-Wallis test, are shown for *$p < 0.05$. In (B – E), the mean deviation of head temperature from ambient temperature ± s.e.m., as measured by thermocouples, is plotted every ten minutes against time (h after midnight). In (F), the temperature of floral faces over three days ± s.e.m, as measured by thermocouples; point estimates on a given day are the averages of three measures taken every five minutes at the beginning, midpoint, and end of a 10 minute interval centered at the times shown. At Morven, one plant per treatment was monitored for three or four days (B, C, F). The period in (C) was characterized by a series of days of inclement weather. In Davis, two plants per treatment monitored for two days in August 2014 (D) and for three days in September 2014 (E). Because malfunction of the ambient data logger at Morven failed to record values for several intervals, some time points on some days were excluded in (B). Because groups of plants were filmed at Morven (A - C, G), pollinator visitations were scored as two types. Initial visits were called when first made to any plant in frame. Additional visits by a pollinator to additional plants in frame were counted toward total pollinator visitations. In Davis (D, E), plants were filmed individually, and this distinction was not required. Bar graphs show mean ± s.e.m. visits per plant in each treatment over n = 3 (A, D) or 4 (B, C, E) days at three times of day (h after dawn). In (G), total pollinator visits were averaged for six plants per treatment; bar graphs show mean ± s.e.m. of these averages over n = 3 days for videos taken at 3 h after dawn. All graphs were plotted in R. Significant differences in pollinator visitation, as determined by t-tests assuming unequal variances, are shown for *$p < 0.05$.

Table S1.

Primers used for gene expression analysis.

Target genes				
Locus	Gene name	Gene sequence	Forward primer	Reverse primer
Ha412v1r1_16g004310	IAA19-like	ATGGGACCTCAGGTGATTGGGCTTGAGATAACTGAACTTAGGTTAGGGCTACCGGGCGGGGGAGCAGTGGTGAGAGAAGAGTGAAGAAGAGGGTGATTTCCGAAGGCGGGCAGGAGGTGGATGTGGTGGTAGGGTGGCCACCGGTGGGGTTGTATAGGAAGAATGTTGTGGCAAAGTTGTACGTGAAAGTGAGCATGGATGGTGTACCGATTCTTAGAAAAGTTGATATAAGTTGTTTTAAAGGGTATTCTGAGCTTGGCATGGGTCTTGAGAAGCTCTTTGATTGTTATGGAATTGGTCAAGCAATGGAAGAAGACAATGGGAGTTGTGAATACACAACAATATATGAAGACAAAGATGGGGATTGGATGCTTGTTGGAGACGTCCCTTGGCTGTAA	ACCGGTGGGGTTGTATAGGA	CGGTACACCATCCATGCTCA
Ha412v1r1_15g036260	LHY-like	CTCGGCTCTCACTCGGCTTTTAATTTTAATTTTAAAATTAAAATTAAAATCTTTATTTTTATTCATCTGCTCTCTTCTTCACACTTCTTCTTCTTTGTTCTTCGTTCTGTTACAGATTTCAATCGATCGATCGATCTAGAAGATTCTGTTAGGACTTCCATCAACGGCTACTGTTGGCACAGTTGCATGATGAAGATGTATGATGAATTATCGTGTTCGTAGTCACTGGATTCGTAGATCGGATGACGAGTTTTGGCATCATCCGGCTCATTTTGTGATAGATTGTCAGGTTTTGTTGAATACTACAACGGCTAAGCTATTTGGATTTGGATTCTACGAGGGGGCTTTTGTATCCCCTACGTGTTCCACAGGATTTGAAGCAGCTGCCATAGATGGACCCCTACTCCTCTGCACCAGGGGAAAATCCTAACATCAAGACTAGAAAACCCTATACGATAACGAAACAACGCGAAAGATGGACAGAGGAGGAGCATAATAGTTTTTTAGAAGCCCTGAAGTTATACGGGCGAGCTTGGCAACGGATAGAAGAACACATAGGAACCAAGACAGCAGTCCAAATCAGAAGTCATGCACAAAAGTTCTTTACAAAGTTGGAAAAGGAGGCTGAAGCTAAAGGAGTTCCAATAAGGCAATCTCTTGACATCGAAATTCCTCCTCCACGCCCTAAACGGAAACCGAGTTATCCGTATCCTCGAAAGACTCGTACTCAGGTGGCAGAAAAGGATGCGAAACCAGCAAGTTTAGTTTCTTCTTTGCAATCACTGGATCTCGAGAGAAAACCTCTTCCCGAGAAAACCAGTCACCAAGAGAAGCTAGAAAACGAAAAAACAAACGAGGAAGCTCAAAATGGTACCACATGTGCATCCTTGTCCTCAGAAAATGAAAATTCCGTACCAAGGTCAAATCATGAAACAAATACATCTTACATCACGATTGAAACTAGAAAGCATCAAGAACTAGATCAAGATGGCATTAAGCACACAAATATTACATCTAATATTTCATTATACGAGAGCTCACACCTTGCGCATGAAAATATCATTCAAGGTCGATATCCTGATATGCCACCTGTGAATCTGATAAACGATACACCCGGTGTGCAGAGTTGTTACCCAAGGCATGTCCCTGTA	TCTGCACCAGGGGAAAATCC	CCTCTGTCCATCTTTCGCGT

		CAAGTCGTAGATGGAAATCATGAATCAACGGTT GATAACTCTGGAGAAGTTCATGATCACCCGAAC CCGTACCTATCTGTTAACATAGCAGCATCTGCA ACTAGTGGCCATCATAATGATGCTACACTTCAT CCTCCTTTCACCCCTTTTAGTGATAATCAAGAG AATTATAGATCGTTTATCCATTTTTCATCGACGA TCTCTAGCCTCATTGTTTCAACTCTGCTACAAAA TCCCGCCGCCCATGCTGCAGCAACCTTTGCAGC TAAATTCTATCATCCCACAAATACGGAAGCTTC CTCCGCAGATTCTTTTTCACGAGATCAGTTGAA TCCTGATACTGGTACTACTCCTAGTATGGCTGC TATTGCTGCTGCTACTATAGAAGCTGCAACTGC ATGGTGGTCCGCTCACGGTCTGCTCCCTGTTTG CGCTCCCTTTTTCCCAGGAGGTTATTTTTGTACA TTTGCGACACCGATAGATGGAAATCAAGCCAAT AACGAACGAGAGAAGGCTCCTTTAGAAGAGAA GATGAATGCAGAAAAGACGGAATCTTCATCAG AGGATGACGACTCTGATGGGAAATTAAATACT GAAGCAAGTCCGGTTGAAACCAAGGAAACGGA AGAAACGGAAACAGTCGTGACTATTCTCGGAA AACCAGTGGACCGGTCTTCTTGTGGTTCTAACA CCATTTCCAGCAGTGAAATGCAAGAAACTAAA GTGTCGGATGTTAATGAGCCTATTTACCGTAGG GGTAGAAGCACTATTAACCCAAACGATTCATGG AAGGAAGTGTCAGAAGAGGGACGACTTGCTTT TCAAGCCCTCTTTTCTAGAGAAGTATTGCCACA AAGCTTTTCTAATGCTCGTACAGTAGCAGAGAA TGATCAACCGAACTGTGAGTTGGACCTAAACAG AACGAGCCAAGAACCTACGGAGAGTAACGGTA ATGAAGGGGTCTTGAGAATGGGAGTGGGGAGT GTGAAGCTGAACGTTCATCATACGGGATTCAAA CCGTACAAAAGGTGTTCGGTTGAGGCTAAAGA AAGCAGCAAGATTATGTGTGCAGGCGGTCAAA ATGATGAGAAAGGTCCAAAGAGAATGTGTTTA GAAACAGAGGAATCAACTTAATTATGAATACA GGACGGGTGTGACTGTTGTATATCATGTTATCC TTACCCTAAAACTCGCTAATCTTATTGTGTAGCT TGTGGGGTTCTATATCTTTTTACATTTTCTGCTG AATATCCACATTGATTATGCTGAATGTATTGGA CTTAATTCTCTTCCTCCTCCTAACCACTGGAGAA TCAAAATTCAACTTCTCGAAAATGCATACTTTC TTTCACCTATCATATCATATGAAGATGCTTCTA GATATTGAATGATGAAATGGTAACACGATGAA AAAAGATTGTAACAACTAAAAGTTCTTACAACC AGATTCGAAATTCCATGCCTTAGCTTTTATAAA CAGGTACCGGAGGCTTGTTTACTGAAGTACTGC TTTGTTTTCGTCCAG		
Ha412v1r1_ 16g045180	SAUR50- like	ATGGGTCTAATCCGAAAGTCACACAAACAAAC TCAAGCACTAGCCATCAAGAAAATCATCAAAA AGTGCTCGAGTTTTGGCAAGAACAACGACGAC AGCGGCCTCCCAAACGATGTCCCAAAAGGACA TTTTGTGGTGTACGTTGGAGAAAGAAGAAACA GATATATTGTTCCGATATCATGTTTGGATCATCC AACATTTCAAGATCTACTACAAAGATCCGAGGA AGAATTCGGATTTAATCACGATATGGGCATCAT	CAAGAA CAACGA CGACAG CG	TCTTTC TCCAAC GTACAC CACA

		CATTCCTTGCCAAGAAGTTGATTTTCTATCTTTT TTCTCCATGATTGCATGA		
Ha412v1r1_ 02g017090	TOC1-like	ATGTTCGGTCCAAAGAAGAGTGAACTAAGGAT AGGTCAGTCTTCAGCCTTTTTTACATATGTCAA ATCGAGCGCGTTCAGGGGTGATACACACGTGG ATGAAGCCAACCCGCCAGCATTAAACATCAAC CCGACCGATGAAAATGCTGCTCGATATGAACAC GCGGTTAGTGATCACGAAAACATATATATCAAT AACGCACCTCGCGATTCGGTATCAGTAGACAGA TCCCCTTTACCTCCAGAATCCAATCTTCAAATG AACTACAACGTATCAGAAACACAACAATCTGG TTATAACCCGTATTCTGCTTATCCATATTACCTA CCGGGACCGATGAACCATGTGATGATGTCACCA GCCTCATCGATGTACCAACAGAACATGAATATT CCACCTCATCACATGCCTGGAATGACATCATTC CCTTACTATCCTGTTAATCTTTGCTTACCTGGCC AGATGCCAGCTGGAATGCCCACATGGCACTCGT ACGGGAATTCTTCTAACCACAATGCGAAGGTAC ATAAACTTGACCGTAGACAAGCAGCTTTGATCA AGTTCAAGCAGAAGAGGAAAGAACGGTGTTTC GATAAGAAAATCAGGTACGTTAATAGGAAAAA GCTAGCAGAGAGACGACCTCGTGTAAGGGGAC AATTTGTGAGGAAGGTTAACGGGATTAATGTGG ATCTTAACGGTCAACCCACTTCTACTGATTTTG ATGATGAGGATGACGACGATGATGATGACGAG GAAGAGGAAGAT	ACCGATG AACCATG TGATGA	TGGCCA GGTAAG CAAAG ATT
Reference genes				
Locus	Gene name	Gene sequence	Forward primer	Reverse primer
Ha412v1r1_ 14g048330	Actin 1-like	CTTCTCTCCCACCTCATTTCTACCGCCATTTTT GCATAATTTATTTCCTCAGGTAAAATTCAACA ATTCCTCTTCATAATGTTGTGTACGCATGTTT ACTTGTTTACAAACTAGGCTTTGGTGCGTCTT AGCATCTAGTGTTTTCATATCTCGTAGAGCGA GGCTTTTGATAGTTTGACAAGGACACCTATAT ATAGGAAGCACCAGCAGCGTATCCACCGTAG CATAAAAGATGGCAGAATCAGAGGACATTCA ACCACTTGTGTGTGATAATGGAACCGGAATG GTTAAGGCTGGTTTTGCTGGAGATGATGCTCC AAGGGCTGTGTTCCCAAGTATCGTTGGCCGA CCACGTCACACTGGTGTAATGGTTGGAATGG GCCAGAAAGACGCTTACGTTGGTGACGAGGC TCAGTCAAAGAGAGGTATTTTGACTTTAAAAT ACCCGATTGAACACGGTATTGTCAGCAACTG GGATGACATGGAGAAAATTTGGCATCACACT TTCTACAACGAGCTCCGTGTCGCCCCAGAAG AACACCCGGTTCTGTTAACCGAAGCGCCTTTG AATCCTAAAGCCAACCGTGAAAAGATGACGC AAATCATGTTCGAGACATTTAACGCACCTGCT ATGTATGTTGCCATCCAAGCTGTTCTTTCTCT CTACGCTAGTGGTCGTACTACTGGTATTGTAC TTGATTCAGGAGACGGTGTGAGCCACACGGT TCCTATATACGAGGGTTACGCTTTGCCACATG CTATCCTCCGGTTGGATCTAGCAGGACGTGAT	CAGCGTA TCCACCG TAGCAT	CCAGCC TTAACC ATTCCG GT

		CTAACCGACTGGTTGATGAAGATTCTAACAG AACGTGGGTATTCATTCACCACAACAGCAGA ACGGGAAATCGTAAGAGACATGAAAGAAAA GCTAGCGTACATCGCTCTAGACTATGAACAA GAGCTCGAGACTTCACAAACTAGCTCTTCTGT TGAGAAGAATTTTGAACTGCCCGACGGGCAG GTCATTACCATCGGTGCTGAGCGTTTCCGCTG CCCGGAGGTGTTGTTCCAGCCGTCTATGATTG GAATGGAAGCAGCTGGTATTCACGAAACCAC ATACAATTCGATCATGAAGTGTGACGTGGAT ATTAGGAAAGATTTGTACGGAAACATTGTGC TTAGTGGCGGTACGACTATGTTCCCCGGGATT GCCGATAGGATGAGCAAGGAAATTACCGCTT TAGCCCCTAGCAGCATGAAGATTAAAGTGGT TGCACCACCCGAAAGAAAGTACAGTGTCTGG ATCGGCGGGTCCATTTTGGCATCACTCAGCAC CTTCCAGCAGATGTGGATTTCAAAGGCGGAA TACGATGAATCCGGTCCATCAATCGTGCACA GGAAGTGTTTCTAAGTCGTTTTGATGAAATTC GATGTTCGATGTTACATGTCATATCTGTTGTT TTGTCGGTGTATTTTTAACTTCCGCAATTCGTT CATTTACTATTTTAGAATCAAGTATTTTGTTT GGAGAATATGATTCCTGTTTTTGATGGTTGAT CTAGTGATGCATTTTGGTGTCATCTTGTTGTG TTTAAACTTCAATTAATTAGTCAGCTGTAAGG TACAATTGGCACATGCATTCTGAAAATGTTCA ACGTGTGGCTAATTATTTGTTTACACAGCATT TAAGCAATACCTTGTGGTAGCAGCTAATGATT GTTACATAGCTTTAAGATTCACCAAACAAGA TGAGATAATGGGTTGCACGTTACAAGATTTTG TTAGAACCTTTGGTGGGTTACTGAAATGGTCC CCCTTGCTTTACGTTTTAA		
Ha412v1r1_11g027330	glyceraldehyde-3-phosphate dehydrogenase of plastid 1-like	TCATAAACAGTAGCAAGCAAGGTCTACCACC ACCACCAGCCGCCGGCCCTTTCTACAACAATC CCCGCCGACCTTTCCCATTTAAATACTCCACA AAGAGCGTTTCTTTAACGCCAAAAGCCATTAT TTTTTCATTCTTATATCTCTCTCTCCCTCTAGG GTTTTGACCATTGCACAAACCCAAACATCTCT ACCAACCCTCCCACATTCATGGCTTCTTTCTC CTCCCTTCTCAGATCCACCAACCCATCACCTG CCCTTCATGCATCCCACCAATCACCCTCCACC CCTACACCATTTCAGGTCTCATCTTTGAAGGT TCAGTCCAACGTGTTTGGTGCTGCTGTTAGTG GGAAATCTTCGTCTTTACAGAAGTCTCATGCA TATAGCATTCAGCCCATCAAAGCTACTGCCAC ACAGACACCAGTTAGTGTTTCAGAGTCCAGC ACAGGTGGGAAGACCAGAGTTGGGATCAATG GTTTTGGAAGAATTGGAAGGTTGGTATTGAG AATAGCAACATTTAGAGATGATATTGAGGTT GTTGCGGTCAATGACCCTTTTATTGATGCCAA GTATATGGCTTACATGTTGAAGTATGACTCTA CTCATGGCCTATTTAAAGGAACTATTAAGGTA GTTGATGAGTCAACTTTGGAAATCAATGGGA AGCAGATAAAAGTATCTAGCCAAAGAGACCC	TGCAATCAAGTACGCCTCTG	TGACCTGGAATCACCAACAA

		AGCAGCGATTCCTTGGGGTGATTTTGGAGCC GACTATGTTGTAGAATCTTCTGGAGTTTTCAC AACGCTTGATAAGGCTTCAGCACACAAGAAG GGTGGTGCCAAGAAGGTGGTGATCTCAGCTC CATCAGCCGATGCACCCATGTTTGTTGTAGGA GTAAACGAGACCACTTACAAGCCAAACATGG ATATCGTATCCAATGCAAGCTGCACCACTAAT TGTTTGGCTCCATTGGCCAAGGTGGTTCATGA AGAGTTCGGTATTGTTGAAGGTTTGATGACA ACTGTCCATGCAACCACAGCGACACAAAAAA CTGTTGATGGACCTTCAATGAAGGATTGGCGT GGAGGTCGTGGTGCTGCACAAAACATCATCC CTAGTTCGACTGGTGCTGCCAAGGCTGTAGG GAAGGTTCTACCAGAACTAAATGGGAAACTA ACGGGTATGGCCTTTAGAGTCCCGACAGCAA ATGTCTCCGTTGTGGATTTAACTTGTCGACTC GAGAAGAACGCTTCTTATGAAGATGTTAAAG CTGCAATCAAGTACGCCTCTGAGGGTCCCAT GCAAGGAATTCTCGGATACACTGATGAGGAT GTCGTCTCCAATGACTTTGTTGGTGATTCCAG GTCAAGTATTTTTGATGCAAAGGCCGGCATA GGGCTAAGTGCATCATTTGTGAAATTGGTGTC GTGGTACGACAATGAGTGGGGTTACAGCAAC CGAGTGTTGGATTTGATCGAGCATATGGCGTT GGTGGCAGCAGCTTCCCACTAAAGGGGAACA TGTTTGTGATTTTTTGTCCTTGCTGTTCTAATA AAAAGGATGGCATAGAATCTTGTTCTGTTTTA TGAACTATTAGAATTCTAGGAAATAAAAGGA TATATGCTTTTGGCATTTGCCACCAGATATGA TTATTTTGGCTTGATTTTTCTCCCATATATCTA CTTAACCAGTCTGATTTACTAGTTTTAAACAG TCTCATTTTAATATCTTCAAGGTTGTCACTGT ATTGACTTATTTCAATATCACAATTTATTTAC TTTATTTTGTTAATTCA		
BQ915612.1	Ribosomal protein L16p-like	TGTTGGACCCGGGATTCGGACTGATGGCCGG ACTGCGGGTGGTATTCTAGAATCTCCCGGAAT ATTAACTCTCTAATATCGTCTTTCGTGACTCTT CGTCTCTCAAACTCAAACTCAAATTTGGAAA ATGACGGACATGACGGCTCGCGTTCGACTTTC GATAGTCCCTTGAAGTAAGAGTCGACGAGTT CCCGTTCTGCGTTCATTTGGTCAGTTGGGAGA AAGAAAATGTCTCAAGTGAAGCACTTGAAGC TGCACGTATCGCATGCAACAAGTACATGACC AAGTTTGCAGGAAAGGATGCTTTCCATTTGA GGGTTAGGGTTCATCCTTTCCACGTGCTTCGT ATCAACAAGATGCTTTCGTGTGCTGGAGCTG ATAGGCTCCAAACTGGTATGAGGGGTGCGTT TGGGAAACCACAAGGTGTCTGTGCTCGTGTA AGCATTGGTCAGGTTCTTCTTTCGGTTCGTTG CAAGGATAACAACAGCCCACATGCTCAAGAG GCCTTGCGTCGTGCTAAGTTCAAGTTCCCTGG GCGTCAAAAGATTATCGTGTCTAGGAAGTGG GGATTCACCAAGTTTAGCCGTACCGACTACAT CCAATGGAAAATCTGAAACCGCATCGTTTCT GACGGTGTTAACGCCAAGCTTCTTGGATGCC	CGGCATG AAGAAG AAAGGA G	TATCAG CTCCAG CACACG AC

		ATGGACCTCT		
Ha412v1r1_13g007230	UBIQUITIN-CONJUGATING ENZYME 21-like	CTCATTTCAACAAAGATATAAAAACACCTCA AGCACATACAGCACATACAAATCGTAGAACG CATCTCTTTTGACTCCATCATCAATTTCTCTCA GGAAGATCACAAATCATATCAAATGCAGGCA TCAAGAGCAAGATTGTTTAAGGAATACAAGG AGGTGCAGAGGGAGAAAGTTGCTGATCCAGA TATTCAGCTTGTTTGTGATGATTCTAATATAT TTAAATGGACTGCACTTATCAAGGGACCGTC AGAAACGCCTTATGAAGGTGGGGTCTTTCAG CTTGCATTTTCTGTTCCAGAGCAATACCCTTT GCAGCCTCCTCAAGTGAGGTTTTTAACCAAA ATATTTCATCCAAATGTACATTTCAAGACGGG AGAAATATGTCTAGATATCCTGAAGAATGCA TGGAGTCCAGCTTGGACGCTCCAGTCTGTTTG TAGAGCTATAATTGCTTTAATGGCCCATCCAG AACCAGATAGCCCTTTAAATTGTGATTCAGG AAATCTTCTTCGATCTGGTGACGTTAGAGGTT TTCAGTCTATGGCTAAGATGTACACCAGGCTT GCAGCGATGCCCAAGAAAGGTTAAAATCATT CATTACTCGCCTTACTTGTGCTTGGTCTCATA TCCACCACCATTGTATGTTTGTGTTACTGCTA TTTTACGGCTTTTGATACTTTTGGTTATGGAA ATTAAGTGTTGTTCAGAACATACACAAATCC AAAGCAAACATTTGCTATTAAACATCATGAA AGTTGTGGTTCATTAGCACAAAGTTAGGTTAA ATAAATGAATCTTTTATTATAATAGTTTTTAC TGAAAACTTATTTGGTTTTCTTTTATGAGAAG AGATCCATTCTGGGCGGATCTATGCAGGCAA CATTTG	GGAGGTGCAGAGGGAGAAAG	TGACGGTCCCTTGATAAGTGC

Movie S1

Heliotropic movement of a young sunflower plant over 24 hours.

Movie S2

Gradual reduction in heliotropic movements as a plant approaches anthesis.

Movie S3

The gibberellin biosynthetic mutant *dw2* only exhibits heliotropism after application of exogenous gibberellin.

Movie S4

Insect visits are more frequent to east- than west-facing flowers.

References

1. L. M. Muller, M. von Korff, S. J. Davis, Connections between circadian clocks and carbon metabolism reveal species-specific effects on growth control. *J. Exp. Bot.* **65**, 2915-2923 (2014).
2. K. Nozue *et al.*, Rhythmic growth explained by coincidence between internal and external cues. *Nature* **448**, 358-361 (2007).
3. K. R. Foster, P. W. Morgan, Genetic Regulation of Development in Sorghum bicolor (IX. The ma3R Allele Disrupts Diurnal Control of Gibberellin Biosynthesis). *Plant Phys.* **108**, 337-343 (1995).
4. L. Jouve, T. Gaspar, C. Kevers, H. Greppin, R. Degli Agosti, Involvement of indole-3-acetic acid in the circadian growth of the first internode of Arabidopsis. *Planta* **209**, 136-142 (1999).
5. A. J. Millar, S. A. Kay, Integration of circadian and phototransduction pathways in the network controlling *CAB* gene transcription in *Arabidopsis*. *Proc. Natl. Acad. Sci. U.S.A.* **93**, 15491-15496 (1996).
6. M. V. Arana, N. Marin-de la Rosa, J. N. Maloof, M. A. Blazquez, D. Alabadi, Circadian oscillation of gibberellin signaling in Arabidopsis. *Proc. Natl. Acad. Sci. U.S.A.* **108**, 9292-9297 (2011).
7. M. F. Covington, S. L. Harmer, The circadian clock regulates auxin signaling and responses in Arabidopsis. *PLoS Biol.* **5**, e222 (2007).
8. C. R. Darwin, *The power of movement in plants*. (John Murray, London, 1880).
9. W. R. Briggs, Phototropism: some history, some puzzles, and a look ahead. *Plant Phys.* **164**, 13-23 (2014).
10. J. P. Vandenbrink, E. A. Brown, S. L. Harmer, B. K. Blackman, Turning heads: the biology of solar tracking in sunflower. *Plant Sci.* **224**, 20-26 (2014).
11. U. Kutschera, W. R. Briggs, Phototropic solar tracking in sunflower plants: an integrative perspective. *Ann. Bot.* **117**, 1-8 (2016).
12. J. H. Schaffner, Observations on the nutation of Helianthus annuus. *Bot. Gaz.* **25**, 395-403 (1898).
13. H. Shibaoka, T. Yamaki, Studies on the growth movement of sunflower plant. *Sci. Pap. Coll. Gen. Educ. Univ. Tokyo* **9**, 105-126 (1959).
14. M. Merrow, M. Brunner, T. Roenneberg, Assignment of circadian function for the Neurospora clock gene frequency. *Nature* **399**, 584-586 (1999).
15. D. Koller, in *Photo-movement,* D.-P. Häder, M. Lebert, Eds. (Elsevier, Amsterdam, 2001), pp. 833-896.
16. M. Fambrini *et al.*, The extreme dwarf phenotype of the GA-sensitive mutant of sunflower, dwarf2, is generated by a deletion in the ent-kaurenoic acid oxidase1 (HaKAO1) gene sequence. *Plant Mol. Biol.* **75**, 431-450 (2011).
17. J. A. Stavang *et al.*, Thermoperiodic stem elongation involves transcriptional regulation of gibberellin deactivation in pea. *Plant Phys.* **138**, 2344-2353 (2005).
18. W. G. Neily, P. R. Hickelton, D. N. Kristie, Temperature and developmental stage influence diurnal rhythms of stem elongation in snapdragon and zinnia. *J. Am. Soc. Hort. Sci.* **122**, 778-783 (1997).
19. H. Ren, W. M. Gray, SAUR Proteins as Effectors of Hormonal and Environmental Signals in Plant Growth. *Mol. Plant* **8**, 1153-1164 (2015).

20. K. Tatematsu *et al.*, MASSUGU2 encodes Aux/IAA19, an auxin-regulated protein that functions together with the transcriptional activator NPH4/ARF7 to regulate differential growth responses of hypocotyl and formation of lateral roots in Arabidopsis thaliana. *Plant Cell* **16**, 379-393 (2004).
21. G. Hagen, T. Guilfoyle, Auxin-responsive gene expression: genes, promoters and regulatory factors. *Plant Mol. Biol.* **49**, 373-385 (2002).
22. A. K. Spartz *et al.*, SAUR Inhibition of PP2C-D Phosphatases Activates Plasma Membrane H+-ATPases to Promote Cell Expansion in Arabidopsis. *Plant Cell* **26**, 2129-2142 (2014).
23. D. Vinterhalter, B. Vinterhalter, J. Miljuš-Djukić, Ž. Jovanović, V. Orbović, Daily changes in the competence for photo- and gravitropic response by potato plantlets. *J. Plant Growth Reg.* **33**, 539-550 (2014).
24. P. G. Kevan, Sun-tracking solar furnaces in high arctic flowers: significance for pollination and insects. *Science* **189**, 723-726 (1975).
25. M. L. Stanton, C. Galen, Consequences of flower heliotropism for reproduction in an alpine buttercup (*Ranunculus adoneus*). *Oecol.* **78**, 477-485 (1989).
26. Y. Ouyang, C. R. Andersson, T. Kondo, S. S. Golden, C. H. Johnson, Resonating circadian clocks enhance fitness in cyanobacteria. *Proc. Natl. Acad. Sci. U.S.A.* **95**, 8660-8664 (1998).
27. A. N. Dodd *et al.*, Plant circadian clocks increase photosynthesis, growth, survival, and competitive advantage. *Science* **309**, 630-633 (2005).
28. A. A. Schneiter, J. F. Miller, Description of sunflower growth stages. *Crop Sci.* **21**, 901-903 (1981).
29. C. A. Schneider, W. S. Rasband, K. W. Eliceiri, NIH Image to ImageJ: 25 years of image analysis. *Nat. Methods* **9**, 671-675 (2012).
30. D. Bates, M. Maechler, B. Bolker, S. Walker, Fitting linear mixed-effects models using lme4. *J. Stat. Softw.* **67**, 1-48 (2015).
31. A. Kuznetsova, P. B. Brockhoff, R. H. B. Christensen, lmerTest: Tests in Linear Mixed Effects Models. R package version 2.0-30. https://CRAN.R-project.org/package=lmerTest, (2016).
32. R. C. Team, R: A language and environment for statistical computing. *R Foundation for Statistical Computing* https://www.R-project.org/, (2015).
33. E. L. Martin-Tryon, J. A. Kreps, S. L. Harmer, GIGANTEA acts in blue light signaling and has biochemically separable roles in circadian clock and flowering time regulation. *Plant Phys.* **143**, 473-486 (2007).
34. J. Vandesompele *et al.*, Accurate normalization of real-time quantitative RT-PCR data by geometric averaging of multiple internal control genes. *Genome Biol.* **3**, RESEARCH0034 (2002).
35. M. V. Matz, MCMC.qpcr: Bayesian analysis of qRT-PCR data. R package version 1.2.2. https://CRAN.R-project.org/package=MCMC.qpcr (2015).